Structures and magic numbers of adatom clusters on metal fcc (001) surfaces

Jun Zhuang,[1,*] Zhihua Sun,[1] Wingham Zhang,[1] Min Zhuang,[2] Xijing Ning,[3] Lei Liu,[1] and Yufen Li[1]
[1]*Department of Optical Science and Engineering, State Key Joint Laboratory for Materials Modification by Laser, Ion and Electron Beams, Fudan University, Shanghai 200433, China*
[2]*Département de Chimie, Université de Montréal, Case Postale 6128 Succursale Centre-ville, Montréal, Québec, Canada H3C 3J7*
[3]*Institute of Modern Physics, Fudan University, Shanghai 200433, China*
(Received 17 September 2003; revised manuscript received 20 January 2004; published 30 April 2004)

With a genetic algorithm, the lowest-energy structures of adatom clusters on a series of metal fcc (001) surfaces are determined. The atomic interactions are modeled by the realistic model potentials including embedded-atom method potential, surface-embedded-atom method potential, and Rosato-Guillopé-Legrand potential. The results show that the adatom clusters of sizes $n=6,9,\ldots,36$ have the same structures on the different surfaces. Their special stability indicates that they are magic number clusters. For clusters of other sizes, the structures are generally different on the different surfaces. The change of the cluster structure with surfaces can be interpreted in terms of the relative interaction range and the compensation effect from the adatom-substrate interaction. When the interaction range becomes long and/or the compensation effect becomes strong, the shape of the lowest-energy structure tends to change from square to rectangle or even to one-dimensional chain.

DOI: 10.1103/PhysRevB.69.165421 PACS number(s): 68.35.Fx, 68.35.Ja

I. INTRODUCTION

The properties of atoms and clusters supported on a surface are basic for understanding many nucleation and growth phenomena. In recent years, considerable work has been devoted to questions of the self-diffusion of adatoms,[1–5] the structure of adatom clusters, and their dissociation and diffusion on metal surfaces.[6–11] To adatom clusters, the lowest-energy structure is one of the basic questions, which reflects fundamental aspects of adatom-adatom and adatom-substrate interactions and provides insights into the initial stages of crystal growth modes. So far a variety of fcc transition and noble-metal surfaces were considered as the substrate, e.g., (110), (001), and (111) surfaces.[12–15] On fcc (001) surfaces, such as Ir/Ir(001) and Pt/Pt(001), an unusual result observed by field ion microscopy is that the stable structures of some small adatom clusters are linear chains instead of close-packed two-dimensional islands.[13,14] The theoretical calculations based on the embedded-atom method (EAM) gave the same result for Pt/Pt(001) system.[14,16] Besides the homogeneous nucleation, e.g., Ni/Ni(001), Cu/Cu(001), and Ag/Ag(001),[17–19] the case of heterogeneous nucleation is also studied extensively, such as Pd/Pt(001), Ni/Pt(001), Pt/Ni(001), and Ni/Al(001), etc.[16,17,20] These studies, however, almost all focus on small clusters. To gain further insight into the related processes such as the early stage of crystal growth, the structure information for larger adatom clusters is usually needed. In addition, it is well known that the magic number cluster behavior has attracted considerable attention in the field of cluster science. The study of the structures of larger adatom clusters can probably lead to the discovery of magic number cluster series and the understanding of the structural features of magic number clusters.

In the present study, the clusters with sizes from $n=2$ to 39 are considered. Following our previous work,[21] an efficient method based on genetic algorithm is used to determine their lowest-energy structures, in which a population of candidate structures is evolved by ''parents'' selecting and mating processes. The metals are modeled by the semiempirical methods. Considering that the semiempirical potentials are probably not exact enough, we perform a systematic study with seven different metals and some different potentials and focus our attention on the generic aspects of the problem.

II. CALCULATION MODEL AND GENETIC ALGORITHM

Seven metals Au, Pt, Ag, Pd, Ni, Cu, and Al are considered. The potentials for modeling these metals include the EAM potential developed by Oh and Johnson,[22] the surface-embedded-atom method (SEAM) potential given by Haftel and Rosen for the surface environment,[23,24] and the potential developed by Rosato, Guillopé, and Legrand (RGL) on the basis of the second-moment approximation to the tight-binding model.[25,26] The aim of using the different potential versions is not to compare their precision. As mentioned above, what we focus on is the generic trends of the structures on the different surfaces. Different potentials and metals provide a variety of possible surfaces or systems, which enables us to perform a systematic study. With the above potentials and metals, eleven different systems, Au(E), Pt(E), Pt(S), Ag(S), Pt(S_0), Ag(E), Ag(R), Pd(E), Ni(E), Cu(E), and Al(E), are obtained, where E and R denote EAM and RGL potentials, respectively, S_0 and S indicate the two SEAM potentials with the different set of the parameters.

The substrates of our systems are (001) slabs of 15 layers thickness, each layer contains 20×20 atoms (40×40 for checking), periodic boundary conditions are applied in the two directions parallel to the surface plane. The bottom four layers are fixed at their ideal bulk values to mimic a semi-infinite crystal, the other layers are allowed to relax to their minimum-energy configuration.

For small adatom clusters, the lowest-energy structure is generally obtained by comparing the relaxed energies of all possible and reasonable structures.[7,15,16] For large adatom

clusters, however, this method is obviously unsuitable because of the large number of the structural isomers. To determine the lowest-energy structure effectively, an optimization method based on the genetic algorithm is used. In our previous work,[21] the details of our optimization strategy were given, which are similar to that developed by Deaven and Ho for free clusters.[27,28] Our method can be summarized as follows.

(1) Create the initial candidate structures randomly for adatom clusters, and relax them to the nearest local minimum. The relaxed candidate structure is characterized by the fitness which in our case is related to the potential energy of the cluster. In the relaxation, the substrate which is relaxed before the cluster is put on is frozen. The candidate structures after the relaxation are indicated by $X_1', X_2', \ldots,$ and X_p', in order of increasing energy. The number of the candidates p is different for the different cluster size n, we take $p=16$ for clusters $n<10$, $p=32$ for $10\leqslant n<25$, and $p=64$ for $n=25-39$.

(2) Select ''parents'' from the population $\{X_1', X_2', \ldots, X_p'\}$ for ''mating''. In order to get a good ''child,'' ''parents'' are selected with a probability $p(X_i')$ depending on their fitness. In the present work, $p(X_i')\propto \exp[-E(X_i')/T_m]$ is adopted, where $E(X_i')$ is the energy of the candidate, and the ''temperature'' T_m is chosen to be roughly equal to the range of energies in the population. In the mating process, a random plane passing through the region of each parent cluster is used to cut the ''father'' and ''mother'' clusters into two parts, respectively. We then join one part of the father to one part of the mother to assemble the ''child'' cluster.

(3), Relax the child to the nearest local minimum on the frozen substrate. If its energy is lower than the highest energy of the candidates in the population and its structure is not identical to that of any candidate, then the child enters into the population and becomes the new candidate. At the same time, candidate X_p' with the highest energy is eliminated from the population for conserving the number of candidates.

(4) Repeat the process from step (2) to (3), which can be regarded as one evolution step, the population $\{X_1', X_2', \ldots, X_p'\}$ then evolves gradually.

(5) In the course of evolution, do full relaxation for the system including the substrate after every certain evolution steps N, where $N=1000n$ is different for different cluster sizes. The cluster structures after every full relaxation are arranged in order of increasing energy and indicated by $\{X_1, X_2, \ldots, X_p\}$. When the structure X_1 with the lowest energy remains unchanged on successive full relaxation, then we think that the lowest-energy structure is reached.

Due to the substrate relaxation, the lowest-energy structure X_1 may not come from the candidate X_1'. For instance, if X_1 comes from the candidate X_5', then it is impossible to get the real lowest-energy structure when the number of candidate structures p is less than 5, even the number of evolution steps is large enough. Therefore, the key point in the above optimization strategy is that the precursor of the real lowest-energy structure X_1 must be included in the final evolved population $\{X_1', X_2', \ldots, X_p'\}$. To verify this point, we double the number of candidate structures p several times for checking. In addition, to obtain the reliable results, we also use the other initial populations by changing the seed for random generator. As expected, the results are not sensitive to the initial population.

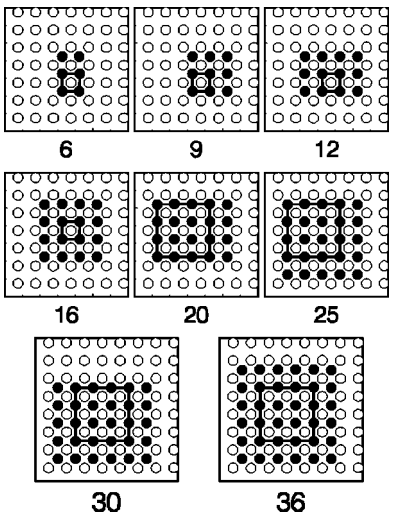

FIG. 1. Structures of the magic number adatom clusters on metal fcc (001) surfaces.

III. MAGIC NUMBERS IN ADATOM CLUSTERS ON fcc (001) SURFACES

Using the above genetic algorithm, we get the lowest-energy structures of adatom clusters with sizes $n=2-39$ on the eleven different surfaces. On Pt(S_0), Ag(E), Ag(R), Pd (E), Ni(E), Cu(E), and Al(E) surfaces, we find that the lowest-energy structures are almost the same for same cluster size. Therefore, in the following, we only report the results on the five surfaces, Au(E), Pt(E), Pt(S), Ag(S), and Pt(S_0), with Pt(S_0) to represent the above seven surfaces. The inner adatom of the cluster has four nearest-neighbor (NN) adatoms (see Fig. 1). In general, it is thought that the four metallic bonds are formed between the adatom and the neighbors. To the border adatom, the number of such NN bonds is less. If we neglect the little difference of these NN bonds, then their total number determines the nearest-neighbor interaction of the cluster. On these surfaces, when the cluster size $n\geqslant 6$, all the lowest-energy structures we obtained are the geometries whose number of NN bonds is maximum. The specific structures, however, are generally different on different surfaces for cluster of the same size. Only the clusters with sizes $n=6,9,12,16,20,25,30,36$ have the same structures on the different surfaces, as shown in Fig. 1, which implies that these clusters are special. Comparing with clusters of other sizes, we find that for each of the clusters with these special sizes there is only one geometry which has the maximum number of NN bonds. This is the reason why they have the same structures on the different surfaces. To see the specialities of these clusters further, in Figs. 2(a) and 2(b), we give the curves of the second finite difference of the energy $\Delta_2 E(n)=E(n+1)+E(n-1)-2E(n)$ on Au(E)

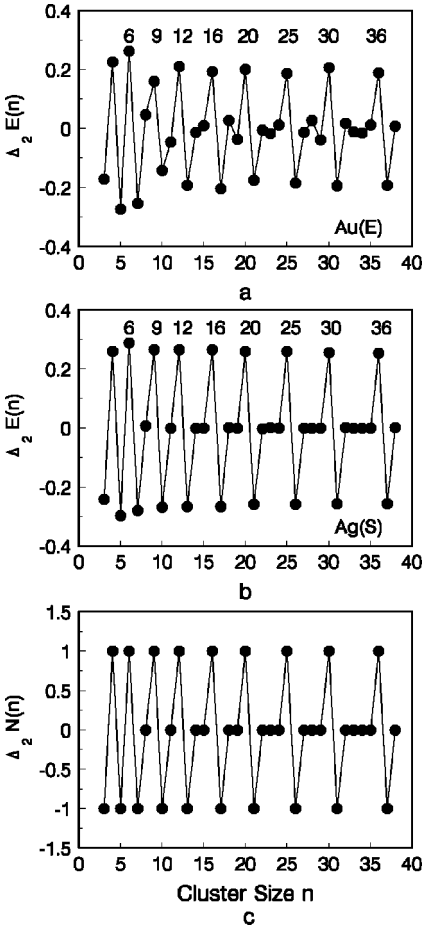

FIG. 2. (a), (b) The second finite difference of the cluster energy on Au(E) and Ag(S) surfaces, respectively. (c) The second finite difference of the number of nearest-neighbor (NN) bonds.

and Ag(S) surfaces, respectively. The curves on the other surfaces are similar to those in the figures. At the sizes $n=6,9,12,16,20,25,30,36$, the large differences $\Delta_2 E(n)$ indicate that the clusters of these special sizes are more stable than their neighbors and can be regarded as magic number clusters. In fact, their outstanding stability can also be seen directly from the structure and the number of NN bonds. Figure 3 is an example on Ag(S) surface, the structure $n=25$ is obviously more perfect than the structures of $n=24$ and 26, and two extra NN bonds are formed when the cluster grows from $n=24$ to $n=25$. From Figs. 1 and 3, we can see that the cluster becomes more stable whenever one side of the outer new quadrangle is completed. Then it is not difficult to imagine the structures of other magic number clusters with sizes $n>36$.

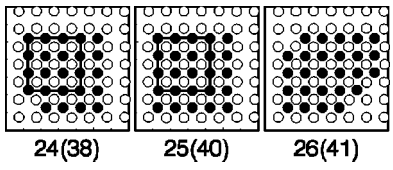

FIG. 3. The lowest-energy structures of clusters $n=24$, 25, and 26 on Ag(S) surface. The number in brackets indicates the number of NN bonds.

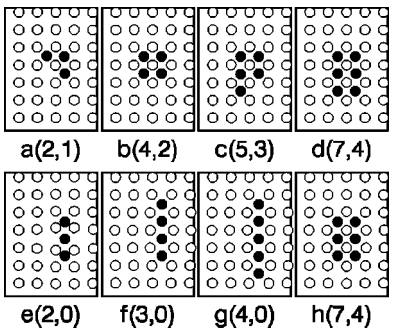

FIG. 4. The lowest-energy structures of clusters $n=3$, 4, 5, and 6 on Pt(S_0) (upper) and Pt(S) (lower) surfaces, respectively. The numbers in brackets indicate the numbers of nearest-neighbor bonds and next-nearest-neighbor bonds (NNN), respectively.

For the clusters $n\geqslant 6$, the result that the structures with maximum number of NN bonds are preferred indicates that the interaction between the nearest-neighbor adatoms dominates the energy of the clusters. For the structures with maximum number of NN bonds, we calculate the second finite difference of their number of NN bonds in Fig. 2(c). The similarity between the two curves in Figs. 2(b) and 2(c) indicates once again that the interaction between the nearest-neighbor adatoms or NN bond is dominant for the cluster energy. In Fig. 2(a), the curve on Au(E) surface deviates a little from that in Fig. 2(c). Similar deviation also exists on Pt(S) surface (the curve is not given in Fig. 2). The deviation indicates that the influence from the adatom-substrate interaction and/or the adatom-adatom interactions beyond the nearest-neighbor range such as the interaction between the next-nearest neighbor adatoms becomes strong. Such influence could lead the lowest-energy structure to take the geometry with fewer number of NN bonds. The cluster $n=4$ on Pt(S) surface is such an example. Similar to the magic clusters $n=6,9,12,\ldots,36$, cluster $n=4$ also has only one geometry which has the maximum number of NN bonds [see Fig. 4(b)]. Consequently, the structure of cluster $n=4$ should be the same on the different surfaces if the NN adatom-adatom interaction is dominant. On surfaces, Au(E), Pt(E), Ag(S), and Pt(S_0), it is indeed true, and Fig. 2(b) indicates that cluster $n=4$ is also a magic cluster. On Pt(S) surface, however, the lowest-energy structure of cluster $n=4$ is different as shown in Fig. 4(f). The reason is the strong influence from the other interactions, the details will be discussed in the following sections. But, as we mentioned above, when the cluster size $n\geqslant 6$ all the lowest-energy structures on the surfaces including Pt(S) are the geometries whose numbers of NN bonds are maximum. This result indicates that for clusters $n\geqslant 6$ the influence from other interactions is not strong enough to change the predominance of the NN adatom-adatom interaction, and then ensures the same magic numbers and same structures of magic clusters on the different surfaces for cluster size $n\geqslant 6$.

In addition, from the structures of the magic number clusters given in Fig. 1, we can imagine the growth mode of the supported clusters on the fcc (001) surfaces we studied. Although the details which we indicate the structures of nonmagic clusters are different on the different surfaces, the

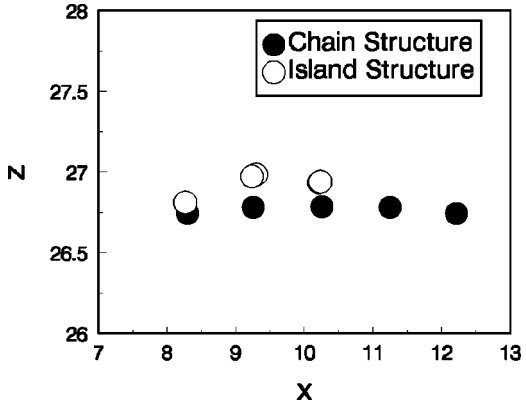

FIG. 5. A side view of the chain and island structures of cluster $n=5$ on Pt(S) surface.

main line of the growth represented by the magic clusters is the same, i.e., growing side by side around a square core.

IV. STRUCTURES OF SMALL ADATOM CLUSTERS

Except the magic clusters, the structures of the other clusters are generally different on the different surfaces. If we describe the structure only in terms of the numbers of nearest-neighbor and next-nearest-neighbor (NNN) bonds, then the structure changes can be classified into two different types. The one is the NN bond related structure change which involves the change of the number of NN bonds. The other is the NNN bond related structure change which involves only the change of the number of NNN bonds. To the surfaces we studied here, the NN bond related structure change only appears in small adatom clusters $n<6$. The examples for clusters $n=4$ and 5 are shown in Fig. 4, from the island structures on Pt(S_0) surface to the linear chains on Pt (S) surface, one NN bond is broken. The fact that the linear chain could become the lowest-energy structure on fcc (001) surfaces, however, is not novel. Similar results were obtained experimentally in Ir/Ir(001) and Pt/Pt(001) systems,[13,14] and in the EAM calculation for Pt/Pt(001).[16] The reason was believed to be the presence of relatively long-range interactions between the adatoms, in which the substrate relaxations play an important role.

In order to give a more clear model for explaining the appearance of the linear chain or the NN bond related structure change with surfaces, we give a side view of the chain and island structures of cluster $n=5$ supported on Pt(S) surface in Fig. 5, in which all atoms including the substrate are fully relaxed. The obvious feature is that the chain is closer to the substrate surface than the island. The difference between the average heights of the adatoms of these two structures is about 0.16 Å. This result implies that the influence from the adatom-substrate interaction on the energy of the chain will be stronger than on that of the island. Then a possible factor accounting for the NN bond related structure change can be given, which is the compensation effect from the adatom-substrate interaction. It is easy to imagine that the chain structure or the structure with fewer NN bonds is generally advantageous to the adatom-substrate interaction due to its weaker internal cohesion and then closer to the surface. In other words, when the number of NN bonds of the structure decreases, the adatom-substrate interaction tends to increase. Therefore, on a certain surface, if such increment of the adatom-substrate interaction is large and can repay the decrement of the NN adatom-adatom interaction because of the NN bond breaking, then the structure with fewer NN bonds could be preferred, e.g., the chain structures of clusters $n=4,5$ on Pt(S) surface. Otherwise, the structure with more NN bonds should be preferred, e.g., the island structures of clusters $n=4,5$ on the other surfaces. Therefore, the strength of the compensation from the adatom-substrate interaction relative to the NN adatom-adatom interaction is one of the key factors for explaining the NN bond related structure change.

To verify the above model, we consider the one-dimensional chain structure and the two-dimensional island structure of cluster $n=5$ supported on Pt(S) surface [for the structures see Figs. 4(g) and 4(c)]. The difference of their cohesive energies (the absolute value of the internal energy) $\Delta E^{2D-1D}=E^{2D}-E^{1D}$ can be regarded approximately as the sum of the differences of the NN adatom-adatom interaction $\Delta E^{2D-1D}_{aa(NN)}$ and the adatom-substrate interaction ΔE^{2D-1D}_{as}, i.e.,

$$\Delta E^{2D-1D}=\Delta E^{2D-1D}_{aa(NN)}+\Delta E^{2D-1D}_{as}. \tag{1}$$

To separate these two kinds of interactions, as the first step, the adatoms of the two structures are fixed in a certain plane whose distance to the first layer is equal to that between the first and second layers of the substrate, and their coordinates x,y are also fixed at the positions as the normal new layer. The substrate which is relaxed before the clusters are put on is frozen. The aim is to exclude the difference resulting from the adatom-substrate interaction between the two structures. Therefore, the cohesive energy difference $E'^{2D}-E'^{1D}$ obtained under this condition approximately comes from the difference of the NN adatom-adatom interaction, i.e., $E'^{2D}-E'^{1D}\approx\Delta E^{2D-1D}_{aa(NN)}$. As one nearest-neighbor bond is broken when the structure changes from the island to chain, the energy difference $E'^{2D}-E'^{1D}$ also approximately equals the cohesive energy of the NN bond E_{NN}, i.e., $\Delta E^{2D-1D}_{aa(NN)}\approx E'^{2D}-E'^{1D}\approx E_{NN}$. Then, releasing all atoms including the substrate, we relax these two structures thoroughly and get the cohesive energy E^{2D}, E^{1D}, and their difference ΔE^{2D-1D}. According to Eq. (1), we can obtain the energy difference $\Delta E^{2D-1D}_{as}=\Delta E^{2D-1D}-\Delta E^{2D-1D}_{aa(NN)}$ which describes the difference of the adatom-substrate interaction between the two structures. The results are shown in Table I, in which the results on other four surfaces are also given. The negative energy difference ΔE^{2D-1D}_{as} indicates that the linear structure is indeed more advantageous to the adatom-substrate interaction than the island structure, and it makes the cohesive energy difference $\Delta E^{2D-1D}=\Delta E^{2D-1D}_{aa(NN)}+\Delta E^{2D-1D}_{as}$ smaller than that before the full relaxation, $\Delta E^{2D-1D}_{aa(NN)}$. In other words, when the NN adatom-adatom interaction decreases in structure change from the island to chain ($\Delta E^{2D-1D}_{aa(NN)}=E'^{2D}-E'^{1D}>0$), the adatom-substrate interaction, however, increases ($\Delta E^{2D-1D}_{as}<0$), that is, the compensation from the

TABLE I. The cohesive energy differences (eV) $\Delta E_{aa(NN)}^{2D-1D}$, ΔE^{2D-1D}, and ΔE_{as}^{2D-1D} between the structures Figs. 4(c) and 4(g) on the different surfaces. $\Delta E_{aa(NN)}^{2D-1D}$ and ΔE_{as}^{2D-1D} approximately come from the differences of the NN adatom-adatom interaction and the adatom-substrate interaction, respectively. ΔE^{2D-1D} is the sum of $\Delta E_{aa(NN)}^{2D-1D}$ and ΔE_{as}^{2D-1D}. E_{NN} indicates the energy of the nearest-neighbor bond.

Surfaces	$\Delta E_{aa(NN)}^{2D-1D}$	ΔE^{2D-1D}	ΔE_{as}^{2D-1D}	$\lvert\Delta E_{as}^{2D-1D}\rvert/E_{NN}$
Pt(S_0)	0.6222	0.5439	−0.0783	0.1258
Ag(S)	0.3287	0.2154	−0.1133	0.3447
Pt(E)	0.4594	0.4534	−0.0060	0.0131
Au(E)	0.2299	0.1371	−0.0928	0.4037
Pt(S)	0.1589	−0.1980	−0.3569	2.2461

adatom-substrate interaction plays a role as expected. $|\Delta E_{as}^{2D-1D}|/E_{NN}$ is the relative compensation, its value $|\Delta E_{as}^{2D-1D}|/E_{NN}>1.0$ on Pt(S) surface for cluster $n=5$ means that for the structure change from the island to chain the cohesive energy increment from the compensation of the adatom-substrate interaction is enough to repay the cohesive energy decrement resulting from the nearest-neighbor bond breaking. Therefore, the linear structure with fewer NN bonds is preferred on Pt(S) surface. On the other surfaces, however, $|\Delta E_{as}^{2D-1D}|/E_{NN}$ is far less than 1.0, which indicates that the compensation is small and cannot repay the cohesive energy decrement resulting from the NN bond breaking. Consequently, all the lowest-energy structures we observed are the geometries with maximum number of NN bonds.

V. STRUCTURES OF LARGE ADATOM CLUSTERS

As mentioned above, another structure change is related to the change of the number of NNN bonds. It appears for clusters $n\geqslant 6$, Fig. 6 is a typical example of this kind of structure change for $n=32$ on the different surfaces. The structures have the same number of NN bonds, $C_{NN}=52$. However, the number of NNN bonds, C_{NNN}, is different, $C_{NNN}=46,45,43$, and 42 for Figs. 6(a), 6(b), 6(c), and 6(d), respectively. That is, from Pt(S_0) surface to Au(E) surface and in sequence Pt(S_0)→Ag(S)→Pt(S)→Pt(E)→Au(E), the number of NNN bonds basically decreases for cluster $n=32$. For other clusters and when the size $n>7$, we find that the numbers of their NNN bonds all tend to decrease on the surfaces in sequence Pt(S_0)→Ag(S)→Pt(S)→Pt(E)→Au(E), i.e., $C_{NNN}[\mathrm{Pt}(S_0)]\geqslant C_{NNN}[\mathrm{Ag}(S)]\geqslant C_{NNN}[\mathrm{Pt}(S)]\geqslant C_{NNN}[\mathrm{Pt}(E)]\geqslant C_{NNN}[\mathrm{Au}(E)]$. Such regular change of the numbers of NNN bonds implies that there is a certain character which is little different on these five surfaces, and it changes monotonically in the sequence Pt(S_0)→Ag(S)→Pt(S)→Pt(E)→Au(E). We will see this character later. In appearance, the decrease of the number of NNN bonds generally makes the shape of the structure change from square to rectangle as the example shown in Fig. 6.

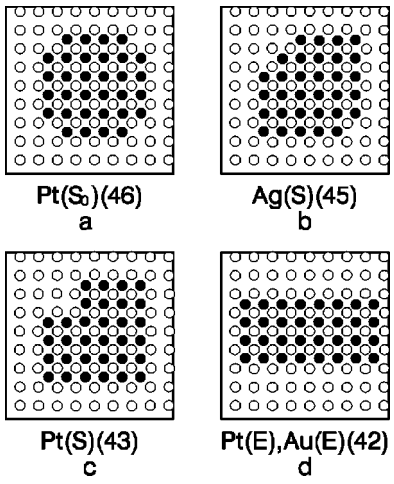

FIG. 6. The lowest-energy structures of cluster $n=32$ on Pt(S_0), Ag(S), Pt(S), Pt(E), and Au(E) surfaces, respectively, in which the number of NNN bonds shown in the brackets decreases from Pt(S_0) surface to Au(E) surface.

TABLE II. The cohesive energy differences (eV) $\Delta E_{aa(NNN)}^{2D-1D}$ and ΔE^{2D-1D} between the structures Figs. 6(c) and 6(d) on the different surfaces. $\Delta E_{aa(NNN)}^{2D-1D}$ approximately comes from the difference of the NNN adatom-adatom interaction, while ΔE^{2D-1D} is the result of the differences of the NNN adatom-adatom interaction and the adatom-substrate interaction.

Surfaces	$\Delta E_{aa(NNN)}^{2D-1D}$	ΔE^{2D-1D}
Pt(S_0)	0.0509	0.0765
Ag(S)	0.0199	0.0140
Pt(S)	−0.0729	0.0115
Pt(E)	−0.0240	−0.0073
Au(E)	−0.0217	−0.0054

Compared with the NN bond related structure change of cluster $n=5$ shown in Figs. 4(c) and 4(g), the structure Fig. 6(a) is the close-packed island analogous to that in Fig. 4(c), and Fig. 6(d) can be regarded as the thick chain structure similar to that in Fig. 4(g). Such similarities motivate us to use the same procedure described in Sec. IV to discuss the physical bases underlying the NNN bond related structure change. The structures used in our calculation are those in Fig. 6(c)(indicated by 2D) and Fig. 6(d) (indicated by 1D). The results are shown in Table II. Cohesive energy difference $\Delta E_{aa(NNN)}^{2D-1D}$ approximately describes the difference of NNN adatom-adatom interaction between the two structures. ΔE^{2D-1D} is the cohesive energy difference between the two structures after full relaxation. Contrary to expectation and opposite to those in Table I, the energy differences ΔE^{2D-1D} after complete relaxation are a little greater than the differences $\Delta E_{aa(NNN)}^{2D-1D}$ except Ag(S). On Ag(S) surface, although the cohesive energy difference decreases from $\Delta E_{aa(NNN)}^{2D-1D}$ to ΔE^{2D-1D}, the decrement is very small and can be neglected. These results mean that there is approximately no compensation from the adatom-substrate interaction when the structure changes from Fig. 6(c) to Fig. 6(d). In other words, the adatom-substrate interactions of the two structures are almost the same, and then the NNN bond related structure change cannot be interpreted by the compensation effect from the

adatom-substrate interaction. Noting that the difference of the number of NNN bonds is one between the structures Figs. 6(c) and 6(d), so $\Delta E^{2D-1D}_{aa(NNN)}$ can be used to estimate the cohesive energy of NNN bond, i.e., $E_{NNN} \approx \Delta E^{2D-1D}_{aa(NNN)}$. Compared with the cohesive energy of NN bond E_{NN}, the magnitude of E_{NNN} is small. In other words, the interaction of NNN adatoms is weaker than that of NN adatoms. Therefore, it is not difficult to understand that the two structures Figs. 6(c) and 6(d) approximately have the same adatom-substrate interaction. We can imagine that when strong bond is formed between the two adatoms, i.e., when the interaction of the two adatoms is strong (e.g., the interaction between the NN adatoms), then they will deviate far from their original equilibrium positions, and the adatom-substrate interaction will be changed greatly. In reverse, if the interaction of the two adatoms is weak (e.g., the interaction between the NNN adatoms), then no matter whether the bond is formed or broken between the two adatoms, the change of the adatom-substrate interaction will be less. Consequently, we cannot distinguish the difference of the adatom-substrate interaction between the two structures from $\Delta E^{2D-1D}_{aa(NNN)}$ and ΔE^{2D-1D} in Table II. The small change from $\Delta E^{2D-1D}_{aa(NNN)}$ to ΔE^{2D-1D} is due to the complete relaxation. So, ΔE^{2D-1D} is approximately the cohesive energy of NNN bond after the complete relaxation. The negative difference ΔE^{2D-1D} on Au(E) and Pt(E) surfaces indicates that the NNN adatoms repel each other. On the other surfaces, Pt(S), Ag(S), and Pt(S_0), however, they attract each other. These results suggest that the NNN bond related structure change as the example shown in Fig. 6 is the result of the different relative interaction range of NNN adatoms. Although it is difficult to determine the relative interaction range exactly, the sign of ΔE^{2D-1D}already shows that the relative interaction ranges on Au(E) and Pt(E) surfaces are longer than those on the others. Consequently, the lowest-energy structures we observed on Pt(E) and Au(E) surfaces are generally more elongated than those on the others. So far the character underlying the regular change of the numbers of NNN bonds, i.e., $C_{NNN}[\mathrm{Pt}(S_0)] \geqslant C_{NNN}[\mathrm{Ag}(S)] \geqslant C_{NNN}[\mathrm{Pt}(S)] \geqslant C_{NNN}[\mathrm{Pt}(E)] \geqslant C_{NNN}[\mathrm{Au}(E)]$ for larger clusters $n>7$ mentioned above, is clear, which is the relative interaction range of NNN adatoms, and the result $C_{NNN}[\mathrm{Pt}(S_0)] \geqslant C_{NNN}[\mathrm{Ag}(S)] \geqslant C_{NNN}[\mathrm{Pt}(S)] \geqslant C_{NNN}[\mathrm{Pt}(E)] \geqslant C_{NNN}[\mathrm{Au}(E)]$ implies that the interaction range tends to increase in the sequence $\mathrm{Pt}(S_0) \rightarrow \mathrm{Ag}(S) \rightarrow \mathrm{Pt}(S) \rightarrow \mathrm{Pt}(E) \rightarrow \mathrm{Au}(E)$.

VI. DISCUSSION

In the above sections, two examples of the structure changes are given. One is the NN bond related structure change of cluster $n=5$, in which we see that the compensation effect of the adatom-substrate interaction plays an important role. Another is the NNN bond related structure change of cluster $n=32$, which is the result of the different relative interaction range of NNN adatoms on the different surfaces. In this section, what we want to supplement is that, to be more precise or to consider some other cases, the two factors, i.e., the compensation effect and the interaction range, in fact determine or influence jointly the lowest-energy structure.

In Sec. IV, the NN bond related structure change of cluster $n=5$ is discussed, in which for simplicity we think that the cohesive energy difference $\Delta E^{2D-1D}_{aa(NN)}$ between the two structures Figs. 4(c) and 4(g) on the frozen surface only comes from their one NN bond difference, the contribution from the different numbers of NNN bonds is neglected, i.e., $\Delta E^{2D-1D}_{aa(NN)} \approx E_{NN}$. The values of $\Delta E^{2D-1D}_{aa(NN)}$ and $\Delta E^{2D-1D}_{aa(NNN)}$ in Tables I and II show that such simplification is reasonable for most surfaces, in which the cohesive energy of NNN bond indicated approximately by $\Delta E^{2D-1D}_{aa(NNN)}$ is far less than the difference $\Delta E^{2D-1D}_{aa(NN)}$. But, to be more precise, $\Delta E^{2D-1D}_{aa(NN)}$ should include the contribution from the NNN bonds. Considering that from the island structure Fig. 4(c) to the chain one Fig. 4(g), three NNN bonds disappear, then $\Delta E^{2D-1D}_{aa(NN)}$ should be written as

$$\Delta E^{2D-1D}_{aa(NN)} = E_{NN} + 3E_{NNN} \approx E_{NN} + 3\Delta E^{2D-1D}_{aa(NNN)}. \quad (2)$$

In other words, the factor of the relative interaction range of NNN adatoms indicated by $\Delta E^{2D-1D}_{aa(NNN)}$ also plays a role in the NN bond related structure change, although its role sometimes is very small. On Pt(S) surface, the contribution $3E_{NNN} \approx 3\Delta E^{2D-1D}_{aa(NNN)} = -0.2187$ eV is larger than those on the other surfaces, in which we use the energy difference $\Delta E^{2D-1D}_{aa(NNN)}$ between the two structures of cluster $n=32$ to estimate the energy of NNN bond. But, it should be noted that the cohesive energy of NNN bond estimated by this method is in fact a kind of equivalent or effective NNN bond energy, it means that such cohesive energy may change a little with the cluster size. Therefore, if we want to get the accurate contribution of the NNN bond to the energy difference $\Delta E^{2D-1D}_{aa(NN)}$ for cluster $n=5$ on Pt(S) surface, we should use the energy difference of the cluster with size close to 5 to estimate the energy of the NNN bond. In Fig. 4, cluster $n=3$ is a good choice, two structures Figs. 4(a) and 4(e) have one NNN bond difference. With these two structures adsorbed on Pt(S) surface, the cohesive energy difference we obtained is $\Delta E^{2D-1D}_{aa(NNN)} = -0.1225$ eV, then the contribution becomes $3E_{NNN} \approx 3\Delta E^{2D-1D}_{aa(NNN)} = -0.3675$ eV. From Eq. (2) and with the value of $\Delta E^{2D-1D}_{aa(NN)}$ in Table I, we can get the cohesive energy of NN bond $E_{NN} \approx 0.5264$ eV, which is basically in accordance with the value 0.51 eV estimated by dissociating the dimer to two single adatoms, and thus verifies the contribution of the NNN bond we give above. The sign of the contribution $3\Delta E^{2D-1D}_{aa(NNN)} < 0$ means that the NNN adatoms repel each other on the frozen Pt(S) surface, and it reduces the cohesive energy difference between the two structures Fig. 4(c) and 4(g) from about $0.5264ev$ to $0.1589ev$, which provides a good condition for the chain geometry Fig. 4(g) to become the lowest-energy structure after the full relaxation or after the compensation effect acts. From this example, we can see clearly that the relative interaction range of NNN adatoms also plays a role in the NN bond related structure change.

With Eqs. (1) and (2), the cohesive energy difference between the two structures after the full relaxation can be further written as

$$\Delta E^{2D-1D}=\Delta N_1 E_{NN}+\Delta N_2 E_{NNN}+\Delta E_{as}^{2D-1D}$$
$$=E_{NN}\left[\Delta N_1+\Delta N_2\left(\frac{E_{NNN}}{E_{NN}}\right)+\left(\frac{\Delta E_{as}^{2D-1D}}{E_{NN}}\right)\right], \quad (3)$$

where ΔN_1 and ΔN_2 are, respectively, the differences of the numbers of NN and NNN bonds between the two structures. With the parameters for cluster $n=5$ on Pt(S) surface, i.e., $E_{NN}\approx 0.5264ev$, $E_{NNN}\approx \Delta E_{aa(NNN)}^{2D-1D}=-0.1225ev$ and $\Delta E_{as}^{2D-1D}=-0.3569ev$, we can estimate approximately the cohesive energy difference ΔE^{2D-1D} for clusters $n=4$ and $n=6$, respectively. For the island and chain structures Figs. 4(b) and 4(f) of cluster $n=4$, $\Delta N_1=1$, $\Delta N_2=2$, we get $\Delta E^{2D-1D}=-0.0755ev<0$ from Eq. (3), which means that the linear chain shown in Fig. 4(f) is the lowest-energy structure on Pt(S) surface. For cluster $n=6$, $\Delta N_1=2$,$\Delta N_2=4$, $\Delta E^{2D-1D}=0.2059ev>0$, which indicates that the island Fig. 4(h) is the preferred structure on Pt(S) surface. These results are all in accordance with those obtained by the genetic algorithm, which thus verifies Eq. (3).

Equation (3) clearly shows that the two factors, i.e., the compensation effect $\Delta E_{as}^{2D-1D}/E_{NN}$ and the interaction range $E_{NNN}/E_{NN}\approx\Delta E_{aa(NNN)}^{2D-1D}/E_{NN}$ jointly determine the cohesive energy difference between the two structures. When $\Delta E_{aa(NNN)}^{2D-1D}$, $\Delta E_{as}^{2D-1D}<0$, the larger the relative magnitudes $|\Delta E_{as}^{2D-1D}/E_{NN}|$ and $|\Delta E_{aa(NNN)}^{2D-1D}/E_{NN}|$ are, the more likely that the linear chain or the geometry with fewer NN bonds becomes the lowest-energy structure. We can imagine that when $|\Delta E_{as}^{2D-1D}/E_{NN}|$ and $|\Delta E_{aa(NNN)}^{2D-1D}/E_{NN}|$ are large enough, then the lowest-energy structure of clusters $n>5$ could also take the linear chain. The typical example is the inhomogeneous nucleation of Ni on Pt(001) surface,[16,17] in which all the lowest-energy structures of clusters $n=3,4,\ldots,9$ are the linear chain. Therefore, although the systems we studied here are limited, the model expressed by Eq. (3) or the physical bases we discussed is helpful for understanding or explaining the appearance of various lowest-energy structures in other cases.

Finally, Eq. (3) is also valid to explain the NNN bond related structure change. In this case, the first term of Eq. (3), $\Delta N_1 E_{NN}$, is zero, and to the surfaces we studied the difference $\Delta E_{as}^{2D-1D}/E_{NN}$ is generally small and can be neglected. Consequently, as we discussed in Sec. V, the relative interaction range of NNN adatoms becomes the dominate factor in determining the lowest-energy structure.

VII. CONCLUSION

On a series of metal fcc (001) surfaces, the lowest-energy structures of adatom clusters ($n=2-39$) are determined by the genetic algorithm. It is found that there is a series of clusters, $n=6,9,\ldots,36$, whose structures are invariable with the different surface. Their outstanding stability indicates that they are magic clusters. Except the magic clusters, the structures of the others generally change with surfaces. For convenience, the structure changes are classified into two different kinds, i.e., the NN bond related structure change and the NNN bond related structure change. The reason for the different structures can be attributed to two factors: the compensation effect from the adatom-substrate interaction and the relative interaction range of NNN adatoms. The NNN bond related structure change (for clusters $n>7$) is mainly due to the different interaction range, while the compensation effect can be neglected. As to the NN bond related structure change, however, the compensation effect is generally significant. On some surfaces, e.g., Pt(S), the interaction range could also play a large role. The longer the interaction range and/or the stronger the compensation effect is, the more likely that the geometry with the fewer NNN bonds and even fewer NN bonds could become the lowest-energy structure, and the shape of the structure tends to change from square to rectangle or even to one-dimensional chain.

ACKNOWLEDGMENTS

This work was supported by Chinese NSF (Grant No. 10004002), ''973'' projection of China (Grant No. 2001CB610506), and the Technology Development Foundation of Shanghai (Grant No. 02QA14007). We acknowledge the usage of facilities at National High Performance Computing Center in Shanghai Research Center for Applied Physics.

*Email address: junzhuang@online.sh.cn

[1] G.L. Kellogg and Peter J. Feibelman, Phys. Rev. Lett. **64**, 3143 (1990).
[2] C.L. Chen and T.T. Tsong, Phys. Rev. Lett. **64**, 3147 (1990).
[3] Jun Zhuang and Lei Liu, Phys. Rev. B **58**, 1173 (1998).
[4] Jun Zhuang and Lei Liu, Phys. Rev. B **59**, 13 278 (1999).
[5] Jun Zhuang, Lei Liu, Xijing Ning, and Yufen Li, Surf. Sci. **465**, 243 (2000).
[6] S.C. Wang and Gert Ehrlich, Surf. Sci. **239**, 301 (1990).
[7] Mark C. Fallis, Murray S. Daw, and C.Y. Fong, Phys. Rev. B **51**, 7817 (1995).
[8] S. Papadia, B. Piveteau, D. Spanjaard, and M.C. Desjonqueres, Phys. Rev. B **54**, 14 720 (1996).
[9] G.L. Kellogg and A.F. Voter, Phys. Rev. Lett. **67**, 622 (1991).
[10] Zhu-Pei Shi, Zhenyu Zhang, Anna K. Swan, and John F. Wendelken, Phys. Rev. Lett. **76**, 4927 (1996).
[11] Jun Zhuang, Qingwei Liu, Min Zhuang, Lei Liu, Li Zhao, and Yufen Li, Phys. Rev. B **68**, 113401 (2003).
[12] H.-V. Roy, P. Fayet, F. Patthey, W.-D. Schneider, B. Delley, and C. Massobrio, Phys. Rev. B **49**, 5611 (1994).
[13] P.R. Schwoebel and G.L. Kellogg, Phys. Rev. Lett. **61**, 578 (1988).
[14] P.R. Schwoebel, S.M. Foiles, C.L. Bisson, and G.L. Kellogg, Phys. Rev. B **40**, 10 639 (1989).
[15] R.C. Longo, C. Rey, and L.J. Gallego, Surf. Sci. **424**, 311 (1999).
[16] Alan F. Wright, Murray S. Daw, and C.Y. Fong, Phys. Rev. B **42**, 9409 (1990).
[17] Chun-Li Liu and James B. Adams, Surf. Sci. **268**, 73 (1992).

[18] M. Breeman, G.T. Barkema, and D.O. Boerma, Surf. Sci. **323**, 71 (1995).
[19] Saroj K. Nayak, P. Jena, V.S. Stepanyuk, W. Hergert, and K. Wildberger, Phys. Rev. B **56**, 6952 (1997).
[20] R.C. Longo, O. Diéguez, C. Rey, and L.J. Gallego, Eur. Phys. J. D **9**, 543 (1999).
[21] Jun Zhuang, Toshitaka Kojima, Wingham Zhang, Lei Liu, Li Zhao, and Yufen Li, Phys. Rev. B **65**, 45 411 (2002).
[22] D.J. Oh and R.A. Johnson, J. Mater. Res. **3**, 471 (1988).
[23] Michael I. Haftel, Phys. Rev. B **48**, 2611 (1993).
[24] Michael I. Haftel and Mervine Rosen, Phys. Rev. B **51**, 4426 (1995).
[25] V. Rosato, M. Guillopé, and B. Legrand, Philos. Mag. A **59**, 321 (1989).
[26] R. Ferrando and G. Tréglia, Phys. Rev. B **50**, 12 104 (1994).
[27] D.M. Deaven and K.M. Ho, Phys. Rev. Lett. **75**, 288 (1995).
[28] Wingham Zhang, Lei Liu, Jun Zhuang, and Yufen Li, Phys. Rev. B **62**, 8276 (2000).